



Reproducible Digital Restoration of Fossils Using *Blender*

Raina P. DeVries^{1*}, Paul C. Sereno^{1,2*}, Daniel Vidal³ and Stephanie L. Baumgart¹

¹Department of Organismal Biology and Anatomy, University of Chicago, Chicago, IL, United States, ²Committee on Evolutionary Biology, University of Chicago, Chicago, IL, United States, ³Grupo de Biología Evolutiva, UNED, Madrid, Spain

OPEN ACCESS

Edited by:

Bruce S. Lieberman,
University of Kansas, United States

Reviewed by:

Denver W. Fowler,
Badlands Dinosaur Museum and
Dickinson Museum Center,
United States
Waisum Ma,
University of Birmingham,
United Kingdom

*Correspondence:

Raina P. DeVries
rpdevries@uchicago.edu
Paul C. Sereno
dinosaur@uchicago.edu

Specialty section:

This article was submitted
to Paleontology,
a section of the journal
Frontiers in Earth Science

Received: 11 December 2021

Accepted: 21 January 2022

Published: 14 February 2022

Citation:

DeVries RP, Sereno PC, Vidal D and
Baumgart SL (2022) Reproducible
Digital Restoration of Fossils
Using *Blender*.
Front. Earth Sci. 10:833379.
doi: 10.3389/feart.2022.833379

Digital restoration of fossils based on computed tomographic (CT) imaging and other scanning technologies has become routine in paleontology. Digital restoration includes the *retrodeformation* and *reconstruction* of a fossil specimen. The former involves modification of the original 3D model to reverse post-mortem brittle and plastic deformation; and the latter involves the infilling of fractures, addition of missing pieces, and smoothing of the mesh surface. The restoration process often involves digital editing of the specimen in ways that are difficult to document and reproduce. To record all actions taken during the digital restoration of a fossil, we outline a workflow that generates both the restored bone and the sequence of steps involved in its retrodeformation and reconstruction. Our method can also generate an animation showing the transformation of the original digital model into its final form. We applied this method to a dorsal rib and frontal bone of a small-bodied Jurassic-age armored dinosaur from Africa, the digital restoration of which engaged all modalities of deformation (translation, rotation, scaling, distortion) and reconstruction (fracture infilling, adding missing bone, surface smoothing). Each bone was CT-scanned, segmented, and imported into *Blender*, an open-source 3D-graphics animation program. *Blender* has an animation tool called an “armature” that allows for precise control over portions of a surface mesh while keeping a record of manipulations. To retrodeform a fossil, an armature is created and then linked, or “rigged,” to the fossil in order to control the displacement and distortion of its fragments. After using the armature to perform retrodeformation, we use *Blender* to record the movement and distortion of each fragment and also record reconstructive modifications. By ensuring documentation and reproducibility in an open-source program, our workflow and output open a window onto the heretofore largely hidden process of digital restoration in paleontology.

Keywords: retrodeformation, reconstruction, blender animation, reproducibility, armature

INTRODUCTION

The fossil bones of vertebrates are rarely preserved in their *in vivo* positions; and individual bones are often deformed, fractured, replaced, or worn down by processes of fossilization, diagenesis, and erosion. Study of these post-mortem agencies is central to the fields of taphonomy (Behrensmeier et al., 2000) and bone diagenesis (Saitta et al., 2019; Ferretti et al., 2021). Even the handling of fossils during excavation, preparation, and study can sometimes inadvertently alter and damage them. During the 19th and 20th centuries, methods used to reverse post-mortem alteration of bones and skeletons included graphical reconstructions, physical repair of bones (sometimes with difficult-to-remove plaster or resin), and mounting original bones with metal armatures or false matrix.

TABLE 1 | Definition of terms used in this paper for the process of digital restoration of a fossil.

Term	Definition	Comments	Software
Digitization	Imaging of a fossil into the form of digital files using scanning technologies.	Includes penetrative (e.g., CT) and surface (e.g., laser) scanning technologies.	Equipment-specific software
Restoration	Digital modification of a fossil to reverse post-mortem alteration.	Includes the delineation, retrodeformation, and reconstruction of a digital rendering of a fossil.	Listed below
Delineation	Surfacing of a fossil with the purpose of rendering it as a mesh model. Delineation is performed after digitization.	Includes the generation of a 3D mesh model of a fossil from a segmented CT image stack or from a surface scan.	3DSlicerMorph, Amira, Avizo, Dragonfly, Mimics (MCS), VGStudio (VGL), Agisoft (PSX)
Retrodeformation	Digital reversal of post-mortem deformation by brittle (translation, rotation) and plastic (scaling, distortion) deformation of the mesh model of a fossil.	Includes reflection, landmark-based repositioning, and form-averaging; but not the addition or subtraction of material.	Blender, ZBrush, R (Morpho)
Reconstruction	Digital addition to or subtraction from a mesh model of a fossil. Involves fracture infilling, the addition of missing pieces, and surface smoothing.	Includes sculpting, hole-filling, island removal, and remeshing.	Blender, ZBrush
Retroanimation	Animation of the digital restoration process.	Includes a sequence of armature poses that show the retrodeformation process leading up to the final restored fossil.	Blender

By the turn of the 21st century, advances in slice-based, computed-tomographic (CT) imaging, surface-based laser scanning, and photogrammetry have revolutionized fossil restoration. Newer methods, such as “vibrational spectroscopy,” are adding to our understanding of the preservation and modification of fossilized tissues (Schopf et al., 2005; Gutiérrez-García et al., 2015; Marshall and Marshall, 2015). Digital images are obtained by increasingly refined scanning methods that capture both the external and internal morphology of fossils, which can then be manipulated digitally for graphical restoration, skeletal articulation, animation of joint excursion or movement, other biomechanical hypothesis testing *in silico* (e.g., examination of stress/strain through finite element analysis), and physical scalable reproduction (Lautenschlager, 2016a; Lautenschlager, 2016b; Lautenschlager, 2017; Kambic et al., 2017; Vidal et al., 2020). Collectively referred to as “virtual paleontology” (Cunningham et al., 2014; Sutton et al., 2014; Sutton et al., 2017), these techniques have transformed the nature of data and analytical tools available to paleontologists interested in reconstructing the skeletal morphology and functions of extinct species.

Terminology and Stages of Digital Restoration

As methods and software packages for digital visualization and modification of fossils have multiplied (Cunningham et al., 2014; Sutton et al., 2014; Sutton et al., 2017), so too have the terms describing these manipulations. We have adapted many of these terms to better suit our workflow, and have provided definitions (Table 1; Figure 1). Note that our workflow is focused on editing the surface mesh of a single fossil. *Digital restoration* is the entire suite of methods applied to a digital scan of a fossil to reverse the effects of taphonomy and restore it to its original *in vivo* condition. After digitization, three stages of digital restoration can be recognized: delineation, retrodeformation, and reconstruction (Figure 1).

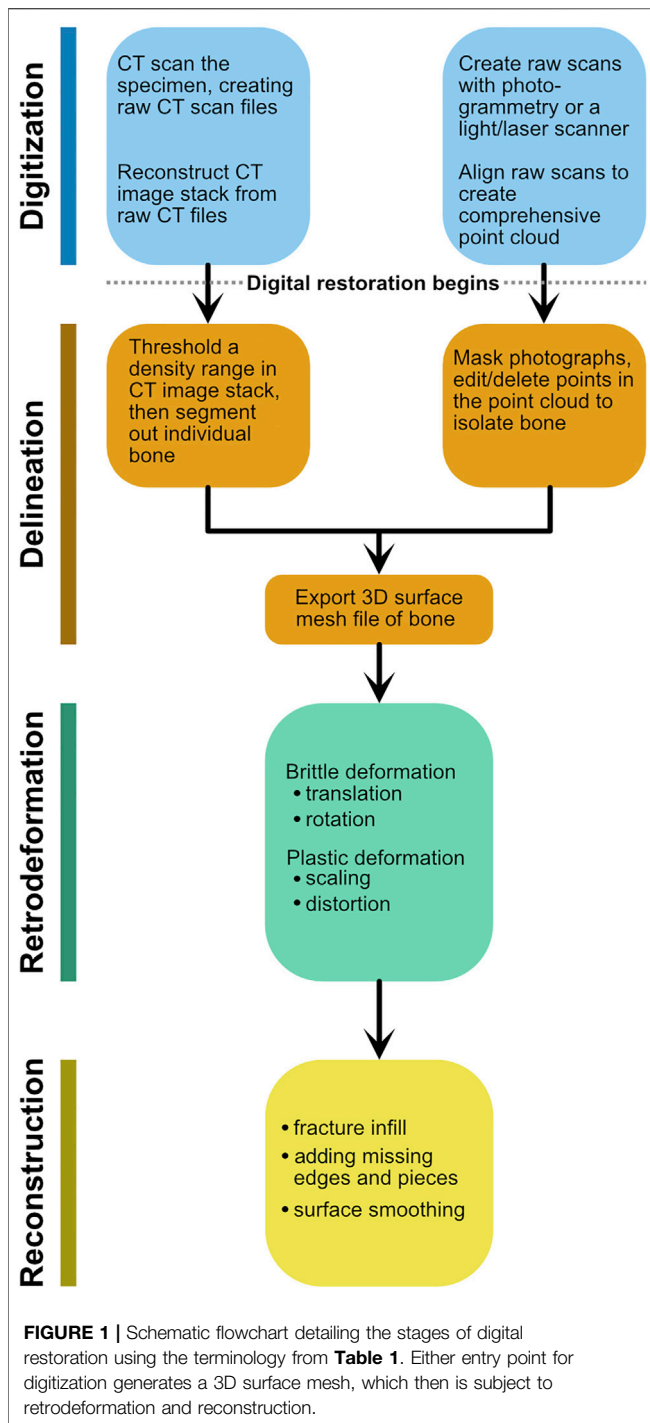
Because digitization does not involve digital alteration of the fossil, it is not included under restoration. Digitization and delineation are performed in sequence. Generally, retrodeformation and reconstruction also occur in sequence, and reconstruction is often viewed as the final and most interpretive stage of digital restoration. A similar workflow was recently outlined for skull restoration (Moya-Costa et al., 2019), although the stages were not named.

Digitization (alternatively referred to as “digitalization”; Moya-Costa et al., 2019) initiates 3D digital restoration by converting a fossil into digital form using either penetrative slice-based scanning methods (Cunningham et al., 2014; Sutton et al., 2014; Lautenschlager, 2016a; Lautenschlager, 2016b; Lautenschlager, 2017; Sutton et al., 2017) or light-based surface scanning methods (Díez Díaz et al., 2021). These processes yield digital 3D files of various formats, which are influenced by settings or parameters during scanning.

The equipment and parameters (metadata) used in a CT scan should be documented and available (Davies et al., 2017), as is now routine (e.g., Morphosource; Boyer et al., 2016).

Delineation involves the surfacing of a digital fossil to generate a 3D mesh model, most often in STL, PLY, or OBJ file formats. Digital model production involves segmentation or editing of the digital fossil to isolate and surface the 3D volume of interest. This initial digital model preserves a pivotal point in digital restoration—the original fossil as it was scanned and surfaced. It documents the starting point, allowing visual comparison and quantification of changes made during the latter two stages of digital restoration. Only rarely, however, is this initial digital model of paleontological specimens documented and made available (Davies et al., 2017). Online repositories, such as Morphosource (<https://www.morphosource.org>) or DataDryad (<https://datadryad.org>), provide access to CT and surface mesh files and are becoming a standard for open science practice involving 3D imaging of fossil and recent specimens.

The focus of this paper is on documenting the stages of digital restoration that are performed on 3D meshes—retrodeformation and reconstruction (Table 1; Figure 1). *Reconstruction* involves



the digital addition to or subtraction from a fossil mesh, including fracture infilling, addition of missing pieces, and smoothing. Retrodeformation was originally coined for the uniaxial or multi-axial deformation of simpler invertebrate shell morphology by geologic processes (Williams, 1990). Currently, retrodeformation can be automated for symmetrical fossils in software (e.g., *R* package *Morpho*; Gunz et al., 2009; Schlager et al., 2018) or automated for fossils with exemplars (Gunz et al., 2009).

The more common retrodeformation process we focus on here, in contrast, involves manual manipulations that are not guided by symmetry or exemplars. These manipulations include the rotation, translation, scaling, and/or distortion of individual fossil fragments that together constitute the retrodeformation process. Manipulations of this type are difficult to record and are therefore rarely documented. Here, using fossilized vertebrate bones as examples, we define *retrodeformation* to include the translation, rotation, scaling, and/or distortion of fragments of a fossil to reverse post-mortem deformation.

Digital Restoration Using *Blender*

Here we use the armatures in *Blender* software to record the movements of fractured pieces (“fragments”) of fossil bones (**Figure 2**) during retrodeformation. *Blender* can sequentially register the repositioning of an armature and its overlying surface mesh, allowing one to document and further capture by animation the process of retrodeformation. In this way, major steps in retrodeformation can be recorded and visualized. Additionally, rotations and the degree of deformation (strain) introduced during retrodeformation can be depicted visually with angle arcs and a 2-color tension map on the final 3D model, respectively.

For reconstruction, the final phase of digital restoration, open-source *Blender* has many of the same “digital sculpting” tools present in commercial software. Digital sculpting tools are often used for infilling gaps, adding missing pieces, and smoothing. In current practice, changes made during digital reconstruction are saved consecutively and, thus, are impossible to reverse beyond the last unsaved iterations. *Blender* software functions similarly. We leave areas of reconstructed bone in gray as an optional color-projection onto the final 3D model.

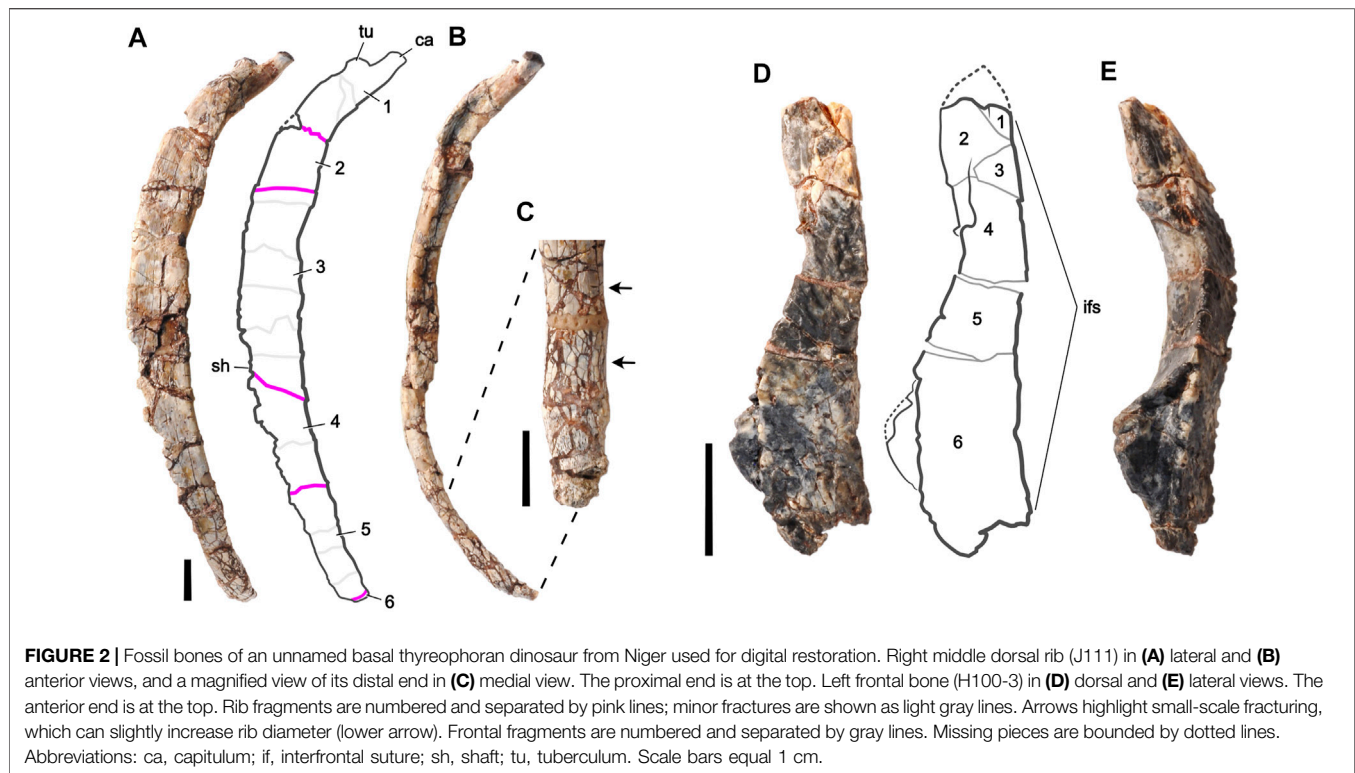
For any restoration of modest complexity, two teams working independently with the same specimen(s) and scan(s) are unlikely to generate precisely the same restored model (Krippner and Peterson, 2017; Moya-Costa et al., 2019). The aim of this paper is to bring transparency, documentation, and reproducibility to the often hidden process of digital restoration in paleontology.

MATERIALS

Example Fossils

The two bones we restored in this study belong to an unnamed, small-bodied, armored dinosaur (early branching thyreophoran) that was excavated in the Jurassic horizons in Niger in 2000 (by PCS; fossils are in the collection of the Musée National Boubou Hama, Niamey, Niger). The fossils were preserved as a disarticulated tangle of bones that were buried together in an overbank deposit of red mudstone in the Tiouraren Formation (Moody and Sutcliffe, 1991; Sereno et al., 1994).

After preparation with pin vise and air scribe, the two bones were scanned at the μ CT facility (PaleoCT) at the University of Chicago (for scan details, see **Supplementary S1**). We segmented the bones with *Amira 2020.2* to generate one triangulated surface mesh per bone (ASCII STL format). The mesh models were then imported—one bone per STL file—into *Blender*.



The fine-grained, compressible matrix of iron-rich (hematitic) mud in which the bones were embedded and the considerable age of the deposit provided ample opportunity during and after fossilization for brittle deformation, displacement of bone pieces with matrix-filled gaps, bone swelling due to small-scale fracturing, and plastic deformation from compressive forces. Most of the deformation is brittle, occurring after the original bone lost most or all of its organic content in the course of fossilization. Thin elongate bones such as ribs are especially susceptible to fracture. Some of the fractures are cut by others, suggesting that several phases of fracturing may be recorded by these bones. Bone surfaces that were smooth in life, such as the major surfaces of the rib, are preserved with texture generated by movement of fragments across a range of sizes. We chose a dorsal rib from the middle of the trunk (Figures 2A–C) and a frontal bone from the skull (Figures 2D,E) that measure 13.4 cm and 4.2 cm in length, respectively.

Fragments and Fracturing

To describe the retrodeformation process, we have divided each bone into numbered pieces, referred to as “fragments,” which exhibit clear evidence of movement from their original position relative to adjacent fragments. Movement of fragments was identified by the *offset edges* of adjacent fragments still in contact and the *matrix-filled gaps* between fragments that had moved apart. The dorsal rib and frontal bone are each composed of six fragments which appear to have moved as brittle pieces as opposed to from plastic deformation (Figures 2A,D).

Minor fractures that separate fragments into smaller pieces (referred to as “fragment parts”) are not offset and do not require

retrodeformation. Minor surface irregularity at a few of these fractures can be removed during reconstruction with smoothing (e.g., remeshing).

Dorsal Rib

During mechanical preparation of the dorsal rib, a few small gaps were filled and bone pieces were glued together where they had separated during cleaning (Figures 2A–C). Fracture surfaces were not cleaned and adjacent fragments were kept in their preserved position. Mechanical retrodeformation was too difficult to effect, and thus, the bone was left as originally preserved. This is the common limit of manual preparation of a fractured or deformed fossil.

Under stereomicroscope and through CT scans, the rib shows little evidence of plastic deformation but considerable evidence of brittle deformation involving the movement of bone fragments. There are five major fractures (pink lines in Figure 2A) that separate the six numbered fragments of the dorsal rib (Figures 2A,B). Movement at these fractures is most suitable to digital restoration. The movement of fragments is neither uniform nor in one direction, as is best seen in the anterior view of the rib (Figure 2B). Some of these fragments are divided into smaller “fragment parts” by fractures that do not involve significant movement (light gray lines in Figure 2A). The surface halfway down the rib shaft shows an oval depressed section where the internal cancellous bone of the rib shaft has collapsed.

The dorsal rib also has small-scale fracturing (Figure 2C). These small-scale fractures are too small and numerous to effectively separate out and recombine. Collectively, they incrementally swell the volume of the bone, a type of

‘explosive’ fracturing that occurs most commonly in pressurized mudstone. Finally, there are several areas of missing bone in the small gaps along fractures and along the thin edges of the rib, some lost during preburial transport and some lost as the result of damage during mechanical preparation of the fragile edges.

Frontal Bone

During mechanical preparation of the frontal bone, several of its fractures were stabilized with glue and fragments were left as they were found. Examining the bone under stereomicroscope and through CT scans confirms the presence of brittle deformation involving the movement of bone fragments. There are five major fractures that separate the six numbered fragments of the frontal bone (Figures 2D,E). Movement of fragments, as with the dorsal rib, is not uniform in only one direction. Small-scale fracturing of the dorsal rib is not present. Two areas of broken bone indicate missing pieces that are present in other frontal specimens (dotted lines in Figure 2D).

Unlike the dorsal rib, the frontal has sustained some plastic deformation, as shown by the dog-legged contour of the interfrontal suture in dorsal view (Figure 2D). This suture is normally a straight sagittal suture with only small-scale interdigitation in dorsal view. Other less complete frontals show the typical planar medial edge of the bone that abuts its opposite in the midline. Most of this deformation appears to have occurred in fragments 4–6 (Figure 2D).

METHODS

Modalities of Retrodeformation and Reconstruction

All modalities of retrodeformation—translation, rotation, scaling, and distortion—were utilized in the digital restoration of at least one of the fossil bones described. For the dorsal rib, retrodeformation involves the *translation* and *rotation* of fragments to reverse brittle deformation. Some fractures require both translation and rotation together to reposition fragments in the original apposition, free of offset edges or gaps (Figures 2A,B). The small-scale fractures of the dorsal rib are filled with very thin sheets of matrix (Figure 2C) which slightly expand the dimensions of the bone in all directions. These fractures can be reversed by incrementally *scaling* down the entire bone by a small amount.

The frontal bone, like the rib, is composed of fragments that have been slightly dislocated (translated, rotated) (Figures 2D,E). Unlike the dorsal rib, however, the frontal shows noticeable signs of plastic deformation. The midline interfrontal suture, which joins the opposing left and right frontal bones of a vertebrate skull, is straight in dorsal view. It deviates only incrementally from the sagittal plane. Other partial frontals of this dinosaur from the same locality have a straight/planar interfrontal suture. The suture in this most complete frontal, however, has a sinuous curve in dorsal view (Figure 2D). That curve appears to be the result of plastic deformation of the bone, a deformation observed in other bones at the site. Reversing that distortion to straighten the medial margin of the frontal requires local plastic reshaping.

In addition to *retrodeformation*, both bones require *reconstruction* to complete the restoration process. The three modalities of reconstruction are fairly distinctive: infilling fractures involves little guesswork; sculpting edges and missing pieces involves approximation from one surface or edge to another and/or modelling unpreserved morphologies on the basis of comparisons with other specimens; and smoothing involves the reduction or simplification of minor surface disturbances and artifacts that are common in fossils. The precise workflow required for each bone is as follows:

Workflow for the Dorsal Rib

Brittle retrodeformation through translation and rotation of fragments was implemented by starting at the proximal end of the bone (fragment 1) and then sequentially moving each successive fragment (fragment 2, 3, 4...) into alignment. Fragment 1 is the frame of reference; all fragments were moved relative to fragment 1. Each fragment movement passively moved those distal to it to maintain their local relations. The retrodeformation and reconstruction of the dorsal rib involved the following eight steps:

- 1) Translate fragment 2 anteriorly and laterally to realign it with fragment 1.
- 2) Translate fragment 3 laterally to realign it with fragment 2.
- 3) Rotate fragment 4 counterclockwise about the dorsal-ventral axis and then translate medially to realign the offset medial edge with fragment 3.
- 4) Translate fragment 5 posteriorly and medially.
- 5) Translate fragment 6 proximally (dorsally and laterally) to close the small gap to fragment 5.

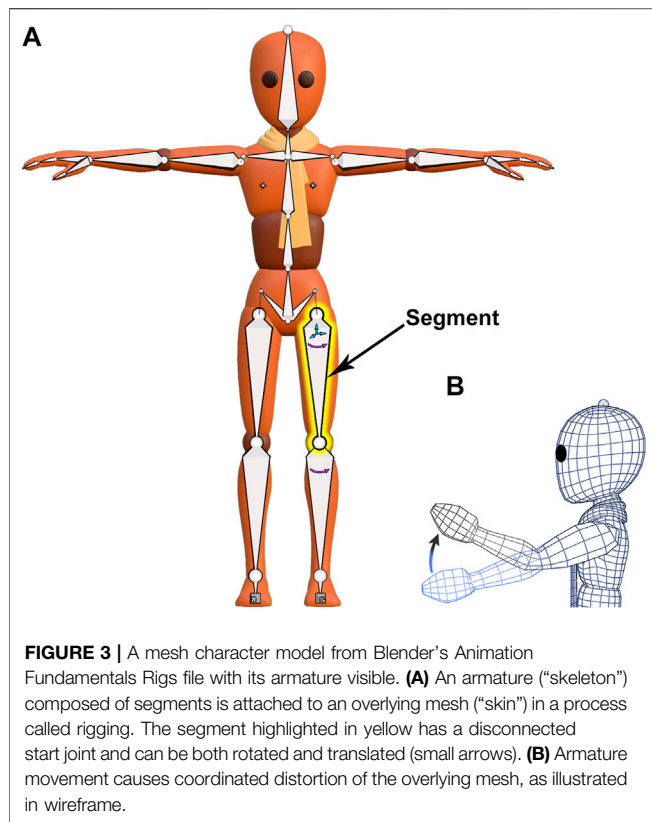
Steps for reconstruction:

- 6) Infill narrow fractures.
- 7) Sculpt missing edges and pieces.
- 8) Smooth the surface of the bone to remove small-scale disturbances.

Workflow for the Frontal Bone

Brittle retrodeformation through translation and rotation of fragments was implemented by starting at the posterior end of the bone (fragment 6) and then sequentially moving each successive (fragment 5, 4, 3...) into alignment. Fragment 6 is the frame of reference; all fragments were moved relative to fragment 6. Each fragment movement passively moved those anterior to it to maintain their local relations. Plastic retrodeformation through distortion of fragments was implemented by starting at the posterior end and then sequentially distorting each successive affected fragment. The retrodeformation and reconstruction of the frontal bone involved the following nine steps:

- 1) Rotate fragment 5 counterclockwise about the dorsal-ventral axis to close the gap to fragment 6.
- 2) Rotate fragment 4 clockwise about the dorsal-ventral axis and then translate laterally to close the gap to fragment 5.



- 3) Rotate fragment 3 counterclockwise about the anterior-posterior axis and then translate laterally to match the medial edge of fragment 4.
- 4) Translate fragment 2 medially and slightly posteriorly and then rotate clockwise about the anterior-posterior axis to align its medial edge with fragment 3.
- 5) Translate fragment 1 laterally and posteriorly and then rotate counterclockwise about the dorsal-ventral axis to align with and also close the gap to fragment 2.
- 6) Plastically deform fragments 6, 5, and 4 in sequence by distorting each fragment about the dorsal-ventral axis to recreate the straight medial edge of the frontal.

Steps for reconstruction:

- 7) Infill narrow fractures.
- 8) Sculpt missing edges and pieces as indicated by the dotted lines (**Figure 2D**).
- 9) Smooth the surface of the bone to remove small-scale disturbances.

Armature-Based Retrodeformation Armatures

Armatures are an animation tool used for posing and animating mesh objects. The armature acts as a "skeleton" with its associated mesh acting as "skin" (**Figure 3A**). A Blender armature is composed of two elements—"bones," termed "segments" (Magrenat-Thalmann et al., 1988) to avoid confusion with

real bones, and "joints." A "segment" (highlighted yellow in **Figure 3A**) has two ball-shaped joints, a "start" joint and an "end" joint. The start joint is the ball on the wider end of the segment and the end joint is the ball on the tapered end. A segment can be rotated about its start joint and additionally can be translated in all three planes if its start joint is disconnected, as with the highlighted yellow segment (small arrows in **Figure 3A**). We will typically associate one segment with one "fragment" in a fossil.

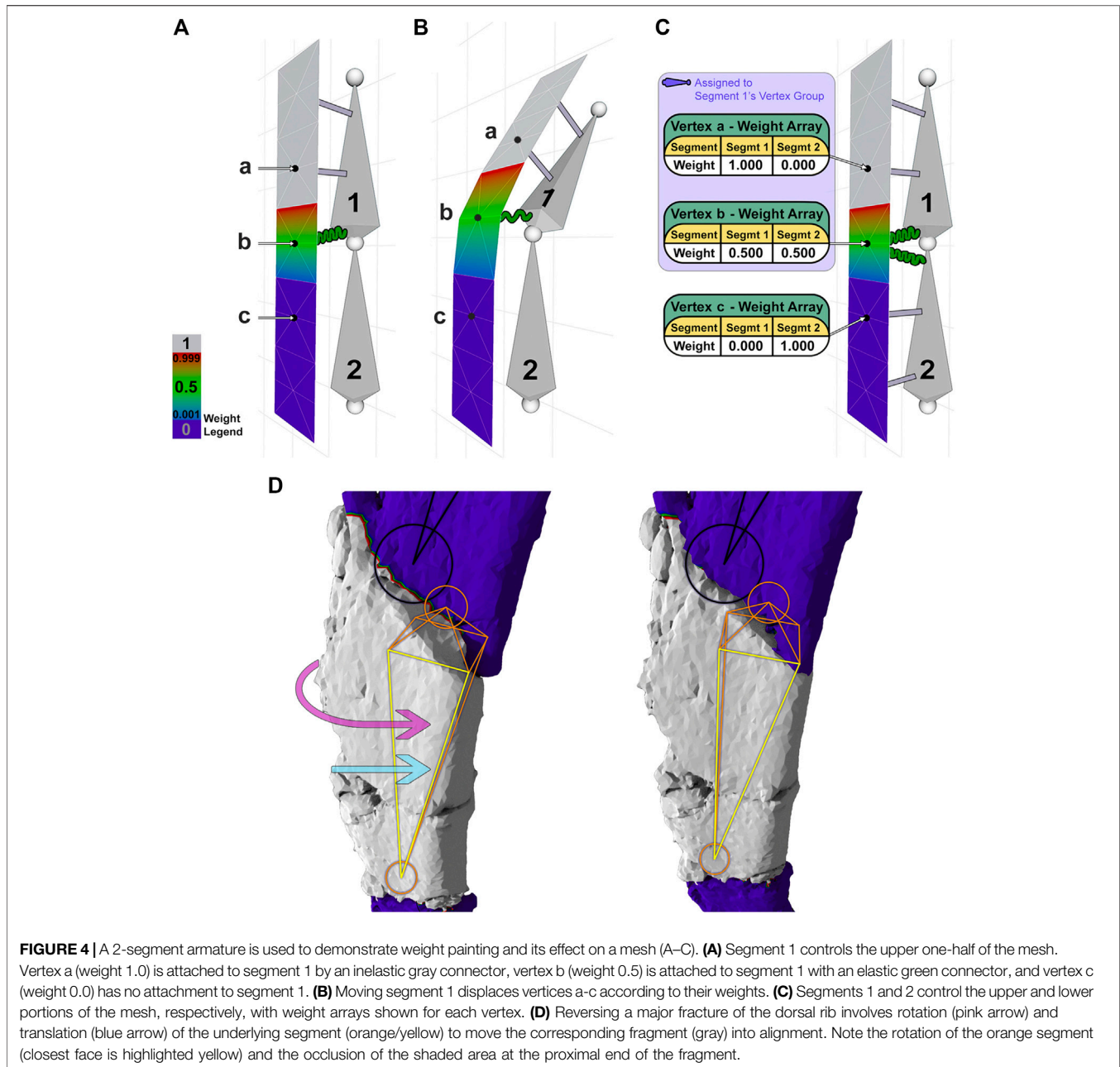
The hierarchical relationship between segments in an armature is useful for the manipulation of fossil fragments. The relationship between consecutive armature segments is described as "parenting." Parenting designates a "parent" object to influence the transforms of a separate "child" object, though the "child" object can still be moved independently. For example, the highlighted yellow segment (**Figure 3A**) is a parent to the segment below it, just as that segment is a parent to the one below it. These predefined relationships cause a segment higher up in the armature hierarchy, a parent, to passively move those that are lower, but not the reverse. Thus, regardless of the order of operations on segments, the armature will always arrive at the same result. A segment with a disconnected start joint can still be parented, as indicated by a dotted line linking its start joint to its parent's end joint (**Figure 3A**). Also, a segment need not lie internal to its associated mesh, although that relation in space is preferred.

The association between armature segments and mesh is strictly defined in a process called "rigging." Once rigged, the movement of armature segments causes the overlying mesh to deform (**Figure 3B**). Armature deformation occurs without loss of positional information and is reversible. Because armature segment transforms (location, rotation, scale) are recorded numerically and their relation to the overlying mesh is specified, animation programs can mass-manipulate associated mesh vertices without loss of the original mesh geometry using armatures. Specific steps to create an armature in Blender are given (**Supplementary S2.A1**). Following armature creation, the connection between segment movement and mesh movement must be specified in a process called weight-painting.

Armature-Mesh Coordination

"Weight painting" is a process used to assign an area of mesh (a "fragment") to a segment in the armature. After assignment, the segment can move, or influence, its assigned area. "Weights" ($0 \leq \text{weight} \leq 1$) describe the level of influence a given segment has over its associated mesh vertices with 0 indicating no influence and 1 indicating a 1:1 relationship. Blender indicates weight values by color-coding the mesh. For this restoration, we have chosen a specific color gradient: indigo (0.000), blue (0.001), green (0.500), red (0.999), and gray (1.000), and the ranges between those colors have intermediate values (Weight Legend in **Figure 4**).

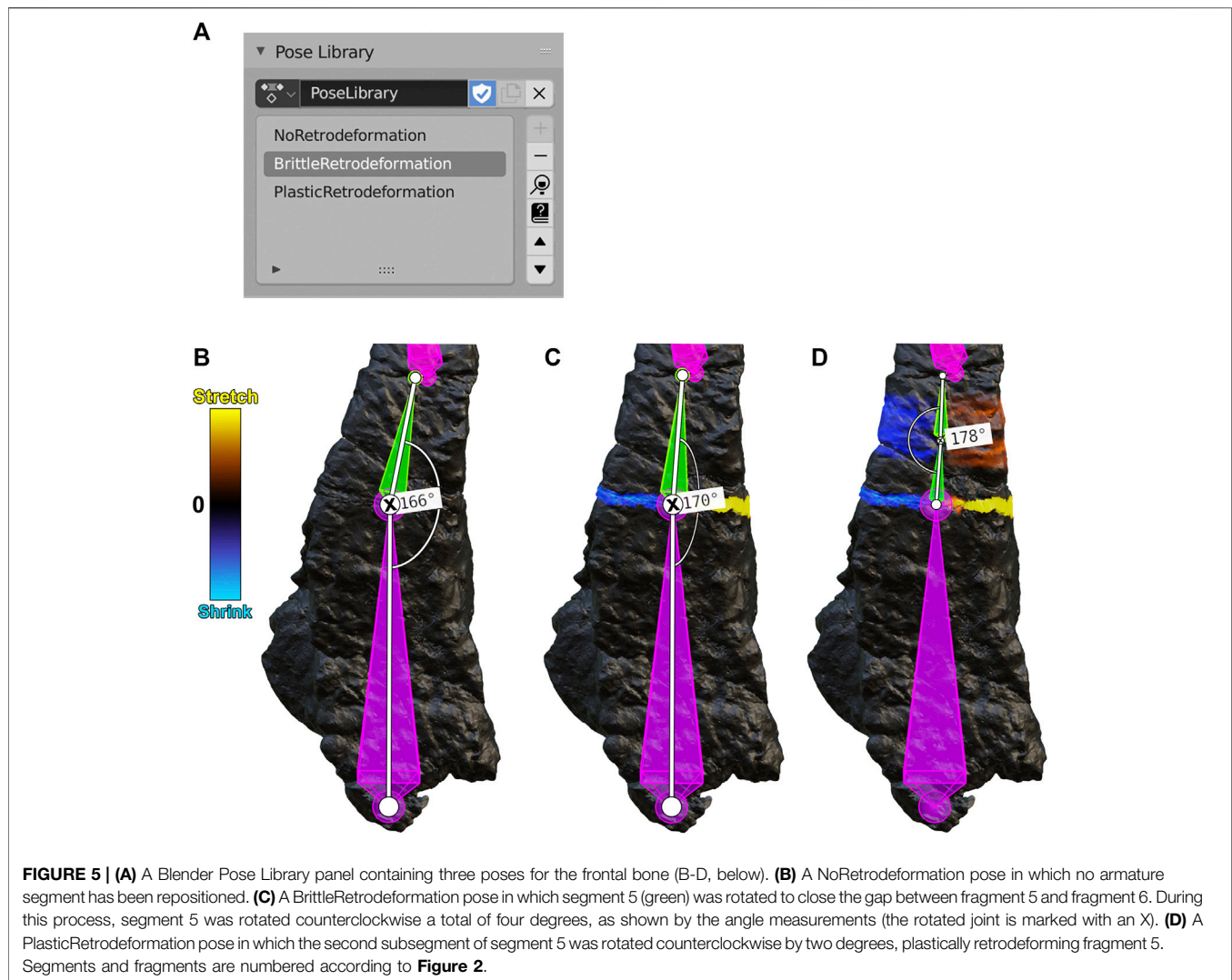
To illustrate the function of weights more clearly, we have created a 2-segment armature that controls a thin slice of mesh. In this example (**Figures 4A,B**), vertex a is connected to segment 1 with a weight of 1.0, visualized by a gray beam, indicating an inelastic connection between this vertex and its segment. Vertex b, in contrast, is connected to segment 1 with a weight of 0.5,



visualized by a green spring, indicating an elastic connection that will move at one-half the rate of its segment. The lower the weight, the less a mesh vertex will move in relation to its connected segment. A single vertex can be assigned weights from multiple segments. For instance (Figure 4C), vertex b is connected to segment 1 with weight 0.5 and segment 2 with weight 0.5, as shown in its associated table or “weight array.” A weight array shows the weights assigned to a vertex per segment, which should sum to 1.0.

Using a section of the dorsal rib containing one major fracture as an example (Figure 4D), an orange/yellow internal segment is connected to the overlying surface mesh corresponding to a

fragment (gray) by inelastic connectors, such that segment rotation (curved pink arrow) or translation (straight light blue arrow) rigidly moves the majority of the fragment without distortion. Narrow zones of mesh corresponding to nearby fractures (red/green/blue) are connected elastically to the segment with weight decreasing across the fracture toward adjacent fragments, which remain uninfluenced (indigo) (Figure 4D). In this case, the red/green/blue borders are vertices connected to consecutive segments. To simulate physical repairs, we have restricted a vertex’s weight array such that it must sum to 1. Thus, each segment has an influence of less than 1 on a shared vertex. A segment’s range



of influence is limited to its “vertex group,” which includes all nonzero vertex connections (light indigo-shaded box in **Figure 4C**). The vertex group of the orange/yellow segment (**Figure 4D**) consists of all non-indigo vertices, showing the complete range of influence of that single segment. The use of vertex groups and weights is how segments are able to manipulate vertices efficiently.

To assign weights to groups of vertices, or “weight-paint,” Blender uses a weight paint brush. For the dorsal rib and frontal bone, the portion of mesh corresponding to a fragment was weight-painted gray (weight of 1) with intermediate weights given to nearby fracture zones. Mesh sections clearly corresponding to another fragment remained indigo (weight of 0) (**Figure 4D**). This process was repeated for each fragment, and corresponding segment, in the armature. Specific steps to weight-paint in Blender are given (**Supplementary S2. A2**). After all fragments of the mesh are weight-painted, each segment in the armature can then be rotated or translated to adjust the shape of the fossil in a process called armature posing.

Armature Retrodeformation

In Blender, “armature posing” refers to the repositioning of segments in an armature to move their corresponding weight-painted fragments. The current position of segments in an armature can be recorded as a “pose.” That pose is then stored in a “Pose Library,” which is a compilation of user-saved poses that can be reapplied to the armature at any time (**Figure 5A**). The stepwise process of retrodeformation (**Figures 5B–D**) can be documented by periodically saving poses to a Pose Library. Here we distinguish between brittle and plastic retrodeformation, the former involving realignment of fragments via translation and rotation and the latter involving distortion of a fragment. In brittle retrodeformation, a given segment is translated and/or rotated to rigidly move its corresponding fragment (**Figures 5B,C**). In plastic retrodeformation, the fragment’s single internal segment can be subdivided and then rotated to best reflect the needed shape change (**Figures 5C,D**). In both brittle and plastic retrodeformation, a segment’s displacement and rotation can

be recorded graphically with Blender's Measure tool (angle measurements in **Figures 5B–D**). Specific steps to pose and measure an armature in Blender are given (**Supplementary S2. A3**). The mesh distortion caused by armature posing can be recorded with a 2-color tension map on the 3D model of the fossil (**Figures 5B–D**). Specific steps to calculate and display a tension map in Blender are given (**Supplementary S2. A7**).

Reconstruction

Reconstruction of fossils often involves sculpting the mesh to infill fractures and/or recreate missing pieces; and smoothing the mesh to repair small cracks and surface disturbances. Blender's sculpting features roughly correspond to those used in other sculpting programs such as ZBrush. Through a combination of sculpting and masking (which prevents sculpting), fractures are infilled and missing parts are reconstructed. After sculpting is finished, these changes are then marked on the sculpted bone by color-projecting a copy of the retrodeformed bone, which is colored non-gray, onto the sculpted one, which is colored gray. In this way, only the reconstructed portions of the sculpted bone will be marked in gray. Specific steps for sculpt-based reconstruction and color projection in Blender are given (**Supplementary S2. A5**). The process of digital restoration is often completed with the smoothing of surface irregularities. We used remeshing to smooth the rib and frontal. Specific steps for remeshing in Blender are given (**Supplementary S2. A6**).

Retroanimation

Retroanimation is defined here as animating the process of digital restoration. To retroanimate in Blender, first, the movements of fossil fragments are animated using an armature, starting with the post-delineation fossil and ending with the retrodeformed fossil. Blender does this by interpolating between user-saved poses, termed "keyframes" in animation, that have been saved in a Pose Library to create a smooth animation sequence of retrodeformation. Next, the retrodeformed fossil is swapped with the reconstructed fossil—both after sculpting additions and after smoothing—to highlight the changes performed during reconstruction. The rendered animation may be stopped, slowed, reversed, or freeze-framed, allowing other researchers to understand the sequence of modifications between the original post-delineation fossil and the final restored fossil. Specific steps for retroanimation in Blender are given (**Supplementary S2. B**). Movies for the retroanimated dorsal rib and frontal bone are available (**Supplementary Movies S1, S2**).

RESULTS

We chose a dorsal rib and frontal bone from a small, armored Jurassic dinosaur for digital restoration. Each bone was examined under magnification and found to consist of six fragments which had moved relative to one another or had suffered distortion. We used Blender's armatures to retrodeform and record fragment manipulations, saving stages of the digital restoration process that we were then able to animate. For each bone, we started

armature-based retrodeformation at one end and then sequentially repositioned successive fragments. Next, we removed any single-fragment distortions. Finally, we sculpted missing pieces and smoothed as needed in the final stage of digital restoration.

Digital Restoration of the Dorsal Rib

We reversed brittle deformation in the dorsal rib, sculpted missing edges, and then smoothed the rib to minimize small cracks and surface disturbances. The dorsal rib showed evidence of brittle deformation, which had split the rib into six fragments. To retrodeform the rib, first, an armature was created and aligned with the dorsal rib such that each segment corresponded to each fragment (**Figure 6A**). Next, the rib was weight-painted to assign each segment to its corresponding fragment. Then, each segment of the armature, starting at the proximal end, was sequentially repositioned to move each fragment of the rib into alignment, performing brittle retrodeformation on the dorsal rib as outlined above (**Figure 6B**).

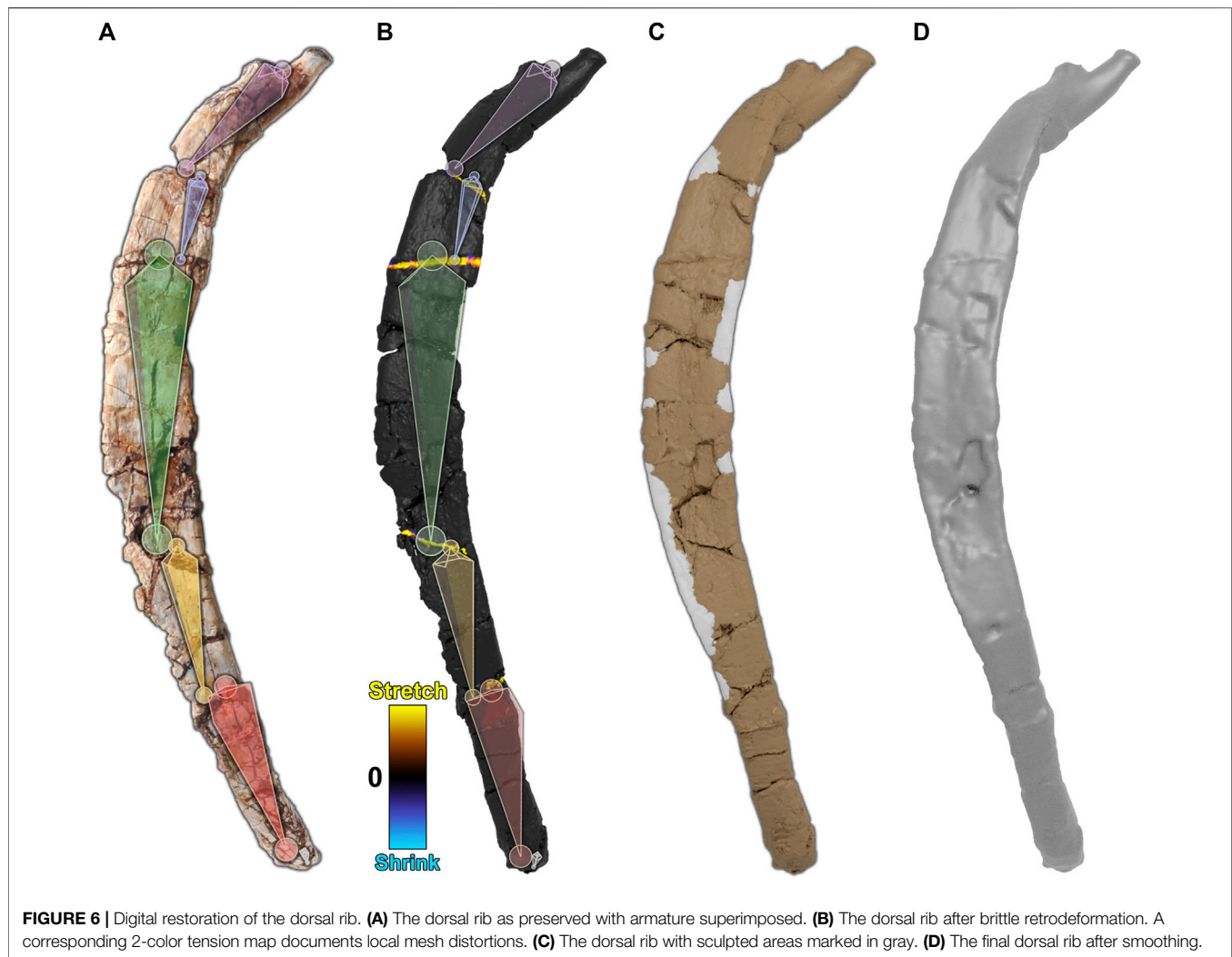
To visualize any mesh deformations that had taken place during segment repositioning, we used a tension map to mark stretched polygons in yellow, shrunken polygons in blue, and unchanged polygons in black (**Figure 6B**). Because the dorsal rib was only subject to brittle retrodeformation, there are only thin bands of yellow polygons visible along the fractures of the rib.

Next, we reconstructed the missing margins of the rib, leaving those areas in gray (**Figure 6C**). Finally, the mesh was smoothed (remeshed) to minimize cracks and surface disturbances (**Figure 6D**). The retroanimation of the dorsal rib restoration is given (**Supplementary Movie S1**).

Digital Restoration of the Frontal Bone

We reversed brittle and plastic deformation in the frontal bone, sculpted missing pieces, and then smoothed the frontal to minimize small cracks and surface disturbances. The frontal bone showed evidence of brittle deformation, which split the frontal into six fragments. Plastic deformation of the bone was also present. To retrodeform the frontal, first, an armature was created and aligned with the frontal bone such that each segment corresponded to each fragment (**Figure 7A**). Next, the frontal was weight-painted to assign each segment to its corresponding fragment. Then, each segment of the armature, starting at the posterior end, was sequentially repositioned to move each fragment of the frontal into alignment, performing brittle retrodeformation on the frontal bone as outlined above (**Figure 7B**). To perform plastic retrodeformation, a second repositioning was required. Fragments that showed signs of plastic deformation first had their segments subdivided. Then, their weights in the mesh regions surrounding the joints formed through subdivision were revised. Finally, the second subsegment of each plastically affected fragment was repositioned to perform plastic retrodeformation (**Figure 7C**).

To visualize any mesh deformations that had taken place during segment repositioning, we used tension maps to mark stretched polygons in yellow, shrunken polygons in blue, and unchanged polygons in black (**Figures 7B,C**). Because the



frontal bone was subject to both types of retrodeformation, there are thin bands of colored polygons at fractures, which correspond to brittle deformation (**Figure 7B**), and accumulated areas of color within plastically affected fragments which correspond to plastic deformation (**Figure 7C**).

Next, we reconstructed the frontal. Missing pieces of the frontal were reconstructed through sculpting. Finally, the mesh was smoothed (remeshed) to minimize cracks and surface disturbances (**Figure 7D**). The frontal bone retroanimation is given (**Supplementary Movie S2**).

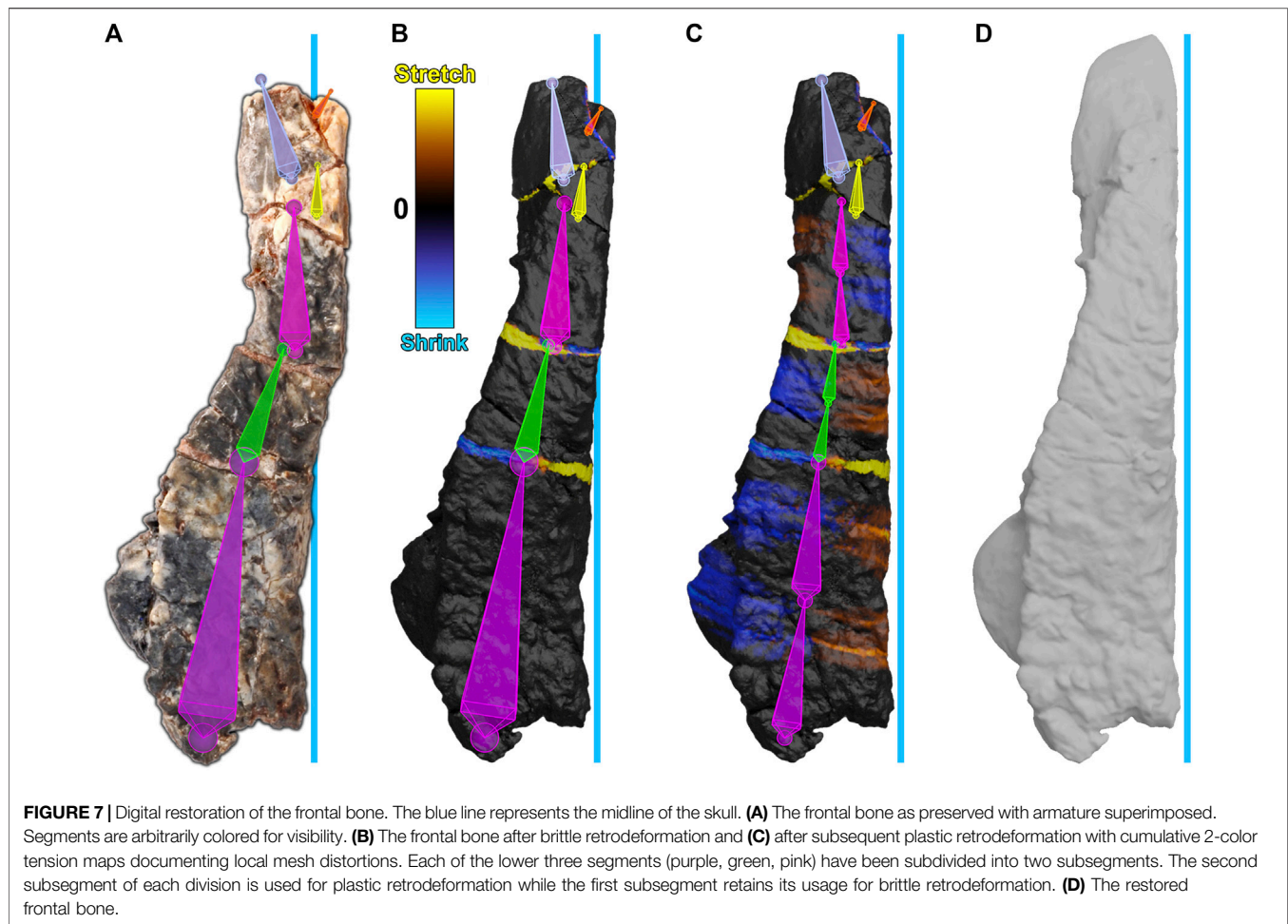
DISCUSSION

We use Blender's armatures, which were created for digital character animation, to manipulate groups of mesh vertices in a controlled and reversible manner as an idealized manipulation of physical bone fragments. We highlight the

potential of armature-based retrodeformation to record the intermediate steps of digital restoration of fossils and to animate the process. Using Blender's armatures, specific manipulations including rotation, translation, scaling, and distortion are accessible to reproduction, evaluation, and critique. Blender is an open-source program, and its use is consistent with the open-science principles of access and reproducibility (Kraker et al., 2011).

Suitability of Armature-Based Retrodeformation

Elongate bones, such as ribs or limb long bones, are well-suited to retrodeformation with armatures because they can be rigged with a single linear armature (with little or no Y-branching). Flat-bones of various shapes can be rigged with a Y-branching armature that allows for more directions of fragment repositioning or distortion correction. More complex bones, such as vertebrae, are more difficult to rig with an armature,



as the armature must accommodate fragments and distortions in multiple directions. In this case, other meshwork such as the manual manipulation of a group of selected vertices via a brush or transformer is the preferred method of retrodeformation.

Challenges of Armature-Based Retrodeformation

Step-specific challenges of armature-based retrodeformation include the effectiveness of segment placement, the complexity of weight-painting, and the transition from retrodeformation to reconstruction. We were able to formulate common-sense rules for segment placement including the idea that the starting number segments should match the number of fragments. However, the centering or positioning of segments within a fragment remains user-dependent. The next step, weight painting, requires preciseness of painting and awareness of active brush settings and vertex groups. Additionally, while Blender contains tools for automatic weighting, the number of polygons in most bone meshes far exceeds the limit. For both segment placement and weight

painting, it may be possible to create new user tools that, for example, calculate the central axis of a fragment or efficiently paint groups of vertices. Another challenge is that Blender's armatures must be removed at the end of retrodeformation to allow reconstruction. Additionally, reconstruction steps must be appended to the retrodeformation animation to create a full record of digital restoration. Thus, integrating standardization and record-keeping for retrodeformation and reconstruction in Blender remains a challenge. These issues are further elaborated elsewhere (**Supplementary S2. C**).

Automated Retrodeformation

Digital restoration of fossils will never be fully automated given the complexity of taphonomic and diagenetic post-mortem processes. Regardless, automation of some steps that are currently entirely manual is desirable for reasons of time, consistency, and objectivity. Current automation methods of retrodeformation use landmark-based geometric morphometrics (GMM) in conjunction with a thin-plate spline (TPS) interpolation algorithm to warp a deformed fossil toward either a bilaterally symmetric average form or an ideal form

(Gunz et al., 2009). Landmarks are points of anatomical significance on a fossil that are identifiable either within species or across similar species; semi-landmarks are points that characterize the curvature of a fossil (Webster and Sheets, 2010).

Landmark-based GMM with TSP is only useful for a minority of fossils, including those that are symmetrical, are represented by many specimens, or have close perfectly preserved extant analogs (Gunz et al., 2009). GMM with TSP is unsuitable for the bones in this study because, as with many fossils, there are few specimens, no close extant analogs, and few suitable landmarks. Future automation of some armature-based retrodeformation steps, nonetheless, is possible and may include: automatic/semi-automatic placement of segments in an armature; automatic weight painting designed for rigid bone fragments; and automatic rotation and translation of segments to align adjacent fragments. Ideal armature-based retrodeformation will likely involve a combination of automated and user-supervised tools.

CONCLUSION

Blender's armatures provide a freely available, open-source means to record and animate stages in the process of digital restoration of fossils, thereby opening these otherwise largely hidden manipulations to scrutiny. The steps taken during digital restoration, which are divided into retrodeformation (translation, rotation, scaling, distortion) followed by reconstruction (fracture infilling, sculpting missing pieces, smoothing), must be better documented and open to evaluation for the process to be regarded as rigorously scientific. We hope the methods outlined here are a step in that direction.

REFERENCES

- Behrensmeyer, A. K., Kidwell, S. M., and Gastaldo, R. A. (2000). Taphonomy and Paleobiology. *Paleobiology* 26 (S4), 103–147. doi:10.1017/s0094837300026907
- Boyer, D. M., Gunnell, G. F., Kaufman, S., and McGeary, T. M. (2016). Morphosource: Archiving and Sharing 3-D Digital Specimen Data. *Paleontol. Soc. Pap.* 22, 157–181. doi:10.1017/scs.2017.13
- Cunningham, J. A., Rahman, I. A., Lautenschlager, S., Rayfield, E. J., and Donoghue, P. C. J. (2014). A Virtual World of Paleontology. *Trends Ecol. Evol.* 29 (6), 347–357. doi:10.1016/j.tree.2014.04.004
- Davies, T. G., Rahman, I. A., Lautenschlager, S., Cunningham, J. A., Asher, R. J., Barrett, P. M., et al. (2017). Open Data and Digital Morphology. *Proc. Biol. Sci.* 284, 20170194. doi:10.1098/rspb.2017.0194
- Diez Díaz, V., Mallison, H., Asbach, P., Schwarz, D., and Blanco, A. (2021). Comparing Surface Digitization Techniques in Palaeontology Using Visual Perceptual Metrics and Distance Computations between 3D Meshes. *Palaentol* 64 (2), 179–202. doi:10.1111/pala.12518
- Ferretti, A., Medici, L., Savioli, M., Mascia, M. T., and Malferrari, D. (2021). Dead, Fossil or Alive: Bioapatite Diagenesis and Fossilization. *Palaogeogr. Palaeoclimatol. Palaeoecol.* 579, 110608. doi:10.1016/j.palaeo.2021.110608
- Gunz, P., Mitteroecker, P., Neubauer, S., Weber, G. W., and Bookstein, F. L. (2009). Principles for the Virtual Reconstruction of Hominin Crania. *J. Hum. Evol.* 57 (1), 48–62. doi:10.1016/j.jhevol.2009.04.004

DATA AVAILABILITY STATEMENT

The original contributions presented in the study are included in the article/**Supplementary Material**, further inquiries can be directed to the corresponding authors.

AUTHOR CONTRIBUTIONS

RD and PS: wrote the initial draft of the paper. RD: conceived of using Blender for digital restoration and generated all digital models. DV and SB: contributed to methods, figures, references, and the text of the final draft.

FUNDING

This research was supported by Bob and Ellen Vladem to PCS at the University of Chicago.

ACKNOWLEDGMENTS

We thank preparator Erin Fitzgerald and students of the University of Chicago for preparation of the fossils and Lauren Conroy and Maria Viteri for CT scanning. For comments on earlier versions of the paper, we thank Evan Saitta.

SUPPLEMENTARY MATERIAL

The Supplementary Material for this article can be found online at: <https://www.frontiersin.org/articles/10.3389/feart.2022.833379/full#supplementary-material>

- Gutiérrez-García, J. C., Gutiérrez-García, T. A., Mosinño, J. F., Vázquez-Domínguez, E., Martínez, A., and Arroyo-Cabrales, J. (2015). A Novel Application of the White Light/Fringe Projection Duo: Recovering High Precision 3-D Images from Fossils for the Digital Preservation of Morphology. *Palaentol. Electronica* 18 (2), 1–13. doi:10.26879/516
- Kambic, R. E., Biewener, A. A., and Pierce, S. E. (2017). Experimental Determination of Three-Dimensional Cervical Joint Mobility in the Avian Neck. *Front. Zool.* 14 (1), 1–37. doi:10.1186/s12983-017-0223-z
- Kraker, P., Leony, D., Reinhardt, W., Gü, N. A., and Beham, n. (2011). The Case for an Open Science in Technology Enhanced Learning. *Ijtel* 3 (6), 643–654. doi:10.1504/ijtel.2011.045454
- Krippner, M. L., and Peterson, J. E. (2017). Comparisons of Fidelity in the Digitization and 3d Printing of Vertebrate Fossils. *J. Paleontol. Tech.* 22, 1–9. doi:10.1130/abs/2017NE-290684
- Lautenschlager, S. (2016a). Digital Reconstruction of Soft-Tissue Structures in Fossils. *Paleontol. Soc. Pap.* 22, 101–117. doi:10.1017/scs.2017.10
- Lautenschlager, S. (2016b). Reconstructing the Past: Methods and Techniques for the Digital Restoration of Fossils. *R. Soc. Open Sci.* 3 (10), 160342. doi:10.1098/rsos.160342
- Lautenschlager, S. (2017). From Bone to Pixel-Fossil Restoration and Reconstruction with Digital Techniques. *Geology. Today* 33 (4), 155–159. doi:10.1111/gto.12194
- Magenat-Thalmann, N., Laperrère, R., and Thalmann, D. (1988). "Joint-Dependent Local Deformations for Hand Animation and Object Grasping," in Proceedings on Graphics interface '88, Edmonton, Alberta, Canada,

- December, 1989 (College of Information Sciences and Technology, Penn. State Univ.), 22–33.
- Marshall, A. O., and Marshall, C. P. (2015). Vibrational Spectroscopy of Fossils. *Palaeontology* 58 (2), 201–211. doi:10.1111/pala.12144
- Moody, R. T., and Sutcliffe, P. J. (1991). The Cretaceous Deposits of the Iullemeden Basin of Niger, Central WestAfrica. *Cretaceous Research* 12, 137–157. doi:10.1016/S0195-6671(05)80021-7
- Moya-Costa, R., Cuenca-Bescós, G., and Bauluz, B. (2019). Protocol for the Reconstruction of Micromammals from Fossils. Two Case Studies: The Skulls of *Beremendia Fissidens* and *Dolinasorex Glyphodon*. *PLoS ONE* 14 (3), e0213174. doi:10.1371/journal.pone.0213174
- Saitta, E. T., Liang, R., Lau, M. C., Brown, C. M., Longrich, N. R., Kaye, T. G., et al. (2019). Cretaceous Dinosaur Bone Contains Recent Organic Material and Provides an Environment Conducive to Microbial Communities. *eLife* 8, e46205. doi:10.7554/eLife.46205
- Schlager, S., Profico, A., Di Vincenzo, F., and Manzi, G. (2018). Retrodeformation of Fossil Specimens Based on 3D Bilateral Semi-Landmarks: Implementation in the R Package "Morpho". *PLoS ONE* 13 (3), e0194073. doi:10.1371/journal.pone.0194073
- Schopf, J. W., Kudryavtsev, A. B., Agresti, D. G., Czaja, A. D., and Wdowiak, T. J. (2005). Raman Imagery: a New Approach to Assess the Geochemical Maturity and Biogenicity of Permineralized Precambrian Fossils. *Astrobiology* 5 (3), 333–371. doi:10.1089/ast.2005.5.333
- Sereno, P. C., Wilson, J. A., Larsson, H. C., Dutheil, D. B., and Sues, H.-D. (1994). Early Cretaceous Dinosaurs From the Sahara. *Science* 266 (5183), 267–271. doi:10.1126/science.266.5183.267
- Sutton, M. D., Rahman, I., and Garwood, R. (2014). *Techniques for Virtual Palaeontology*. Chichester, West Sussex, UK: John Wiley and Sons.
- Sutton, M., Rahman, I., and Garwood, R. (2017). Virtual Paleontology—An Overview. *Paleontol. Soc. Pap.* 22, 1–20. doi:10.1017/scs.2017.5
- Vidal, D., Mocho, P., AberasturiSanz, A. J. L., Sanz, J. L., and Ortega, F. (2020). High Browsing Skeletal Adaptations in Spinophorosaurus Reveal an Evolutionary Innovation in Sauropod Dinosaurs. *Sci. Rep.* 10, 6638. doi:10.1038/s41598-020-63439-0
- Webster, M., and Sheets, H. D. (2010). A Practical Introduction to Landmark-Based Geometric Morphometrics. *Paleontol. Soc. Pap.* 16, 163–188. doi:10.1017/s1089332600001868
- Williams, S. H. (1990). Computer-Assisted Graptolite Studies. In Editors D. L. Bruton and D. A. T. Harper. *Microcomputers in Palaeontology, Contributions from the Palaeontology Museum*. Oslo: University of Oslo.

Conflict of Interest: The authors declare that the research was conducted in the absence of any commercial or financial relationships that could be construed as a potential conflict of interest.

Publisher's Note: All claims expressed in this article are solely those of the authors and do not necessarily represent those of their affiliated organizations, or those of the publisher, the editors and the reviewers. Any product that may be evaluated in this article, or claim that may be made by its manufacturer, is not guaranteed or endorsed by the publisher.

Copyright © 2022 DeVries, Sereno, Vidal and Baumgart. This is an open-access article distributed under the terms of the Creative Commons Attribution License (CC BY). The use, distribution or reproduction in other forums is permitted, provided the original author(s) and the copyright owner(s) are credited and that the original publication in this journal is cited, in accordance with accepted academic practice. No use, distribution or reproduction is permitted which does not comply with these terms.